Supporting information to Chemical Communications

A simple tactic synthesis of hollow porous graphitic carbon nitride with significantly enriched photocatalytic performance

Vellaichamy Balakumar [a]*, Ramalingam Manivannan [b], Chitiphon Chuaicham [a], Sekar Karthikeyan [a] and Keiko Sasaki [a]*

[a] Department of Earth Resources Engineering, Faculty of Engineering, Kyushu University, 744 Motooka, Nishiku, Fukuoka 819-0395, Japan

[b] Department of Advanced Organic Materials Engineering, Chungnam National University, 220 Gung-dong, Yuseong-gu, Daejeon 305-764, South Korea

Corresponding authors: *

E-mail: keikos@mine.kyushu-u.ac.jp, (Prof. Keiko Sasaki), Tel: +81-92-802-3338, ORICD id: http://orcid.org/0000-0002-2882-0700 & kumar@mine.kyushu-u.ac.jp (Vellaichamy Balakumar)

S1. Experimental section

S1.1 Synthesis of CN

CN was fabricated via the thermal polycondensation method. First, 4.0 g of urea was placed into a sealed crucible and calcined at 550 °C for 4 h in a muffle furnace with a heating rate of 10 °C min^{-1}. After calcination, CN was obtained as a yellow solid product. A similar procedure was adopted to synthesize porous CN with a heating rate of 100 °C min^{-1}.

S1.2 Photocatalytic experiments

Photocatalytic degradation of CIP using both the synthesized CN sheet and porous structure was performed under visible light ($\lambda > 420$ nm) irradiation. First, 50 ml of 10 ppm CIP and 50 mg of catalyst material were magnetically stirred under dark conditions for 10 min to reach adsorption-desorption equilibrium. The suspensions were irradiated using a 500 W Xe lamp with a cut-off filter. Samples were collected and filtered (0.45 μm membrane filters) at different time intervals to check the absorbance using UV-Vis spectrometry at a wavelength of 272 nm. Further, sample degradation was measured and confirmed by HPCL. The photocatalytic degradation rate for the reaction was calculated using Eq. (1):

$$-\ln C_t/C_0 = kt \quad (1)$$

where k is the rate constant and C_0 and C are the concentrations of CIP at reaction times of 0 s and t, respectively.

Table S1 The informations of instrumentation used for characterization and analysis study

Instrument	**Model/Make**	**Study**
UV–DRS spectroscopy	Shimadzu UV-2450 spectrophotometer	Absorbance properties
FT-IR spectroscopy	Jasco FTIR-670 Plus, Japan	Identification of functional groups
X-ray diffraction	Rigaku Ultima IV diffractometer	Crystalline structure
SEM, EDX and mapping analysis	SEM; FlexSEM-1000 with Oxford instruments (EDX)	Surface morphology and elemental compositions
HR-TEM analysis	HR-TEM; JEOL JEM-2100HCKM	Structure and surface morphology
Surface area analysis	BEL-Max N_2 porosimeter	Specific surface area of materials
X-ray photoelectron spectroscopy	ULVAC-PHI ESCA 5800	surface compositions and states
Solid state photoluminescence spectroscopy	PL; JASCO F-6600	Photoluminescence properties
Ultra-high-performance liquid chromatography-mass spectrometry	UHPLC-MS (1290 infinity II/ Qtrap 6500	Analysis of intermediate degradation products
Electrochemical experiments	Solartron analytical (1280C Electrochemical test system)	Photocurrent and impedance analysis

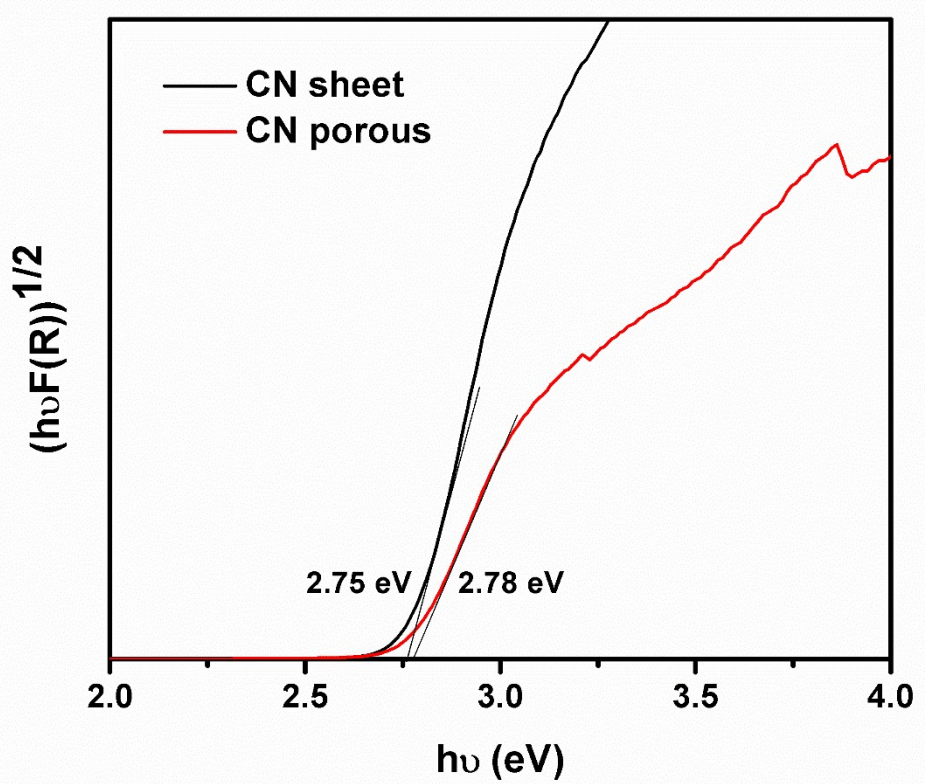

Fig. S1 Plots between $(h\nu F(R))^{1/2}$ vs. hν (eV) for synthesized sheet and porous CN.

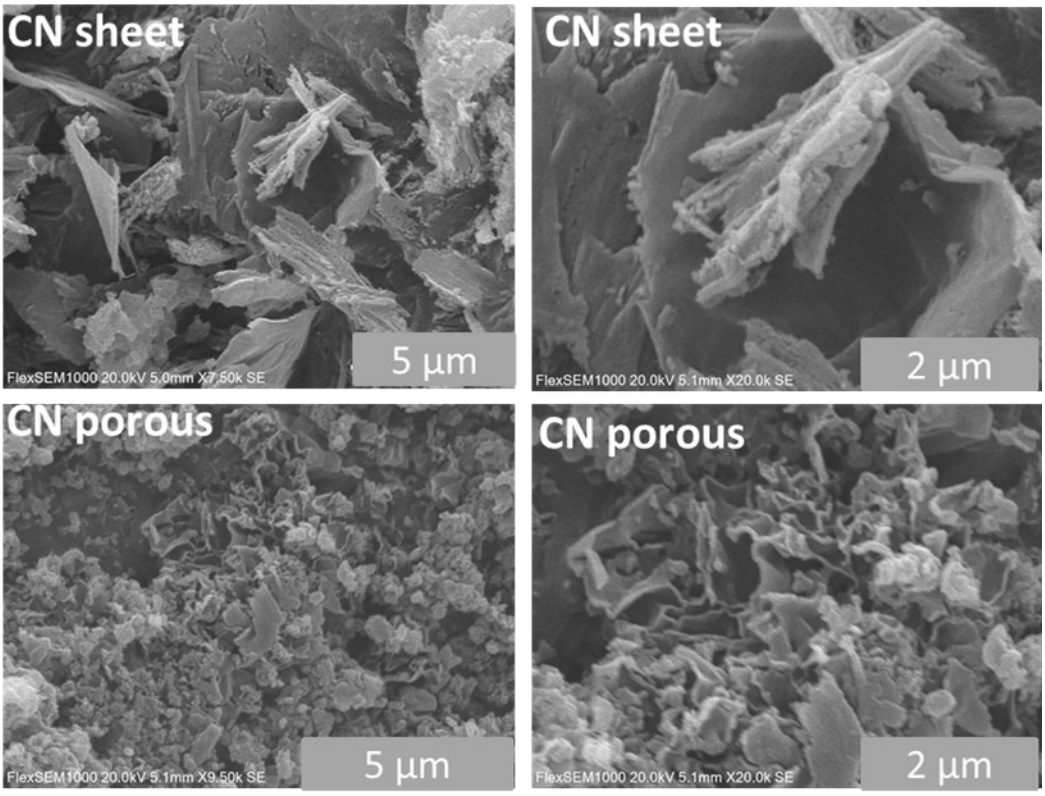

Fig.S2 Different magnifications SEM images of sheet and porous CN.

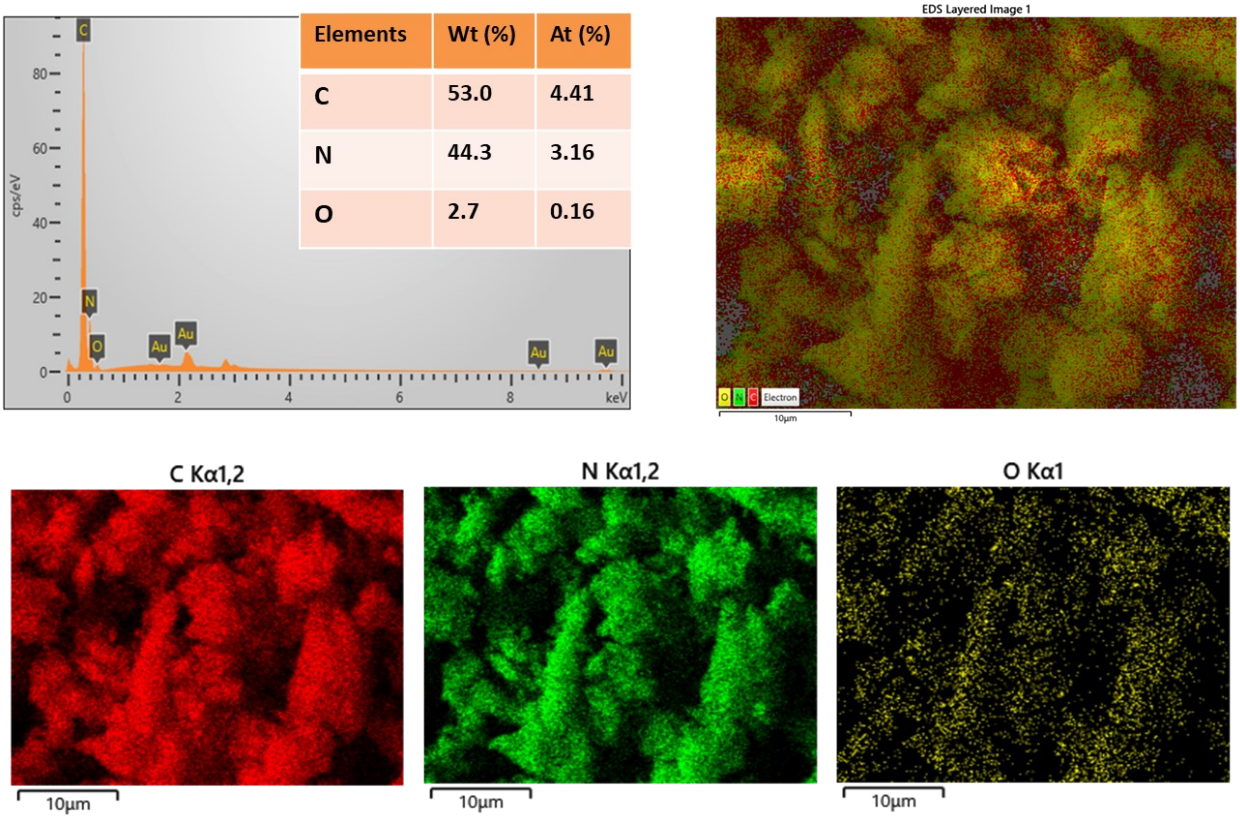

Fig. S3 EDX and mapping analysis of sheet CN.

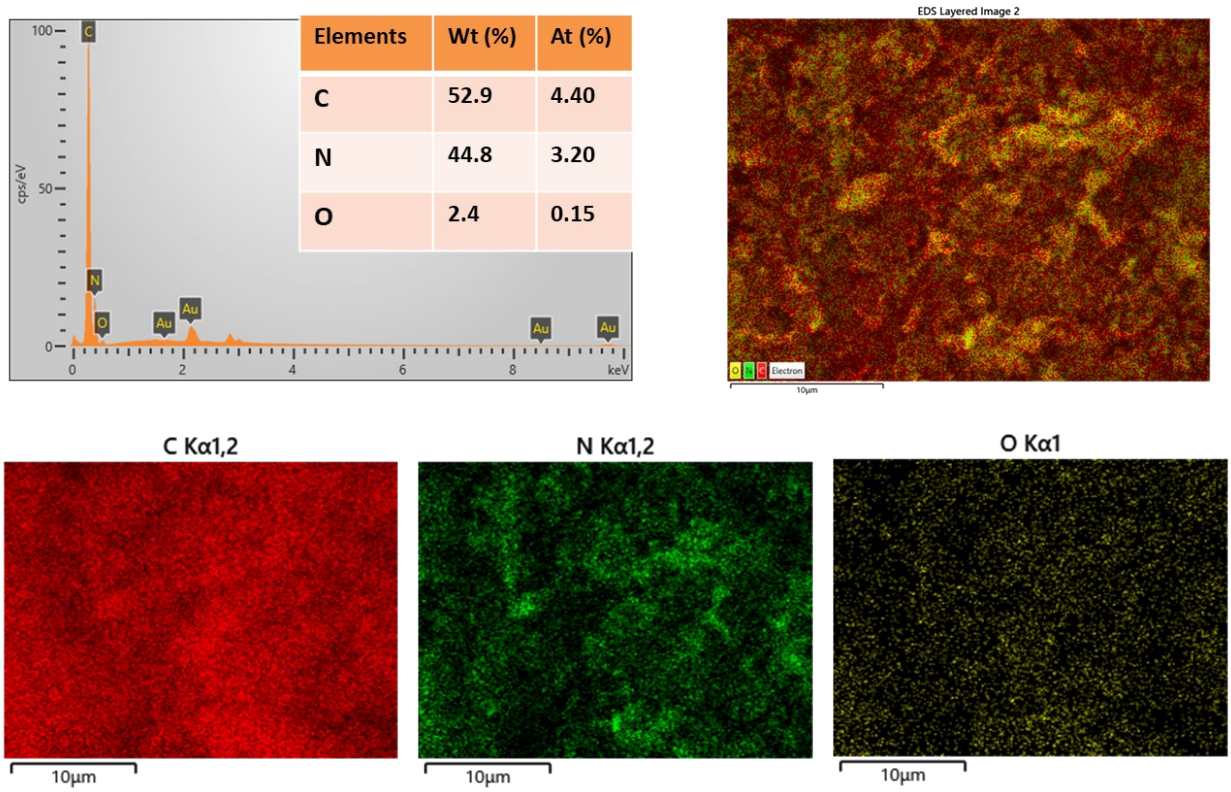

Fig. S4 EDX and mapping analysis of porous CN.

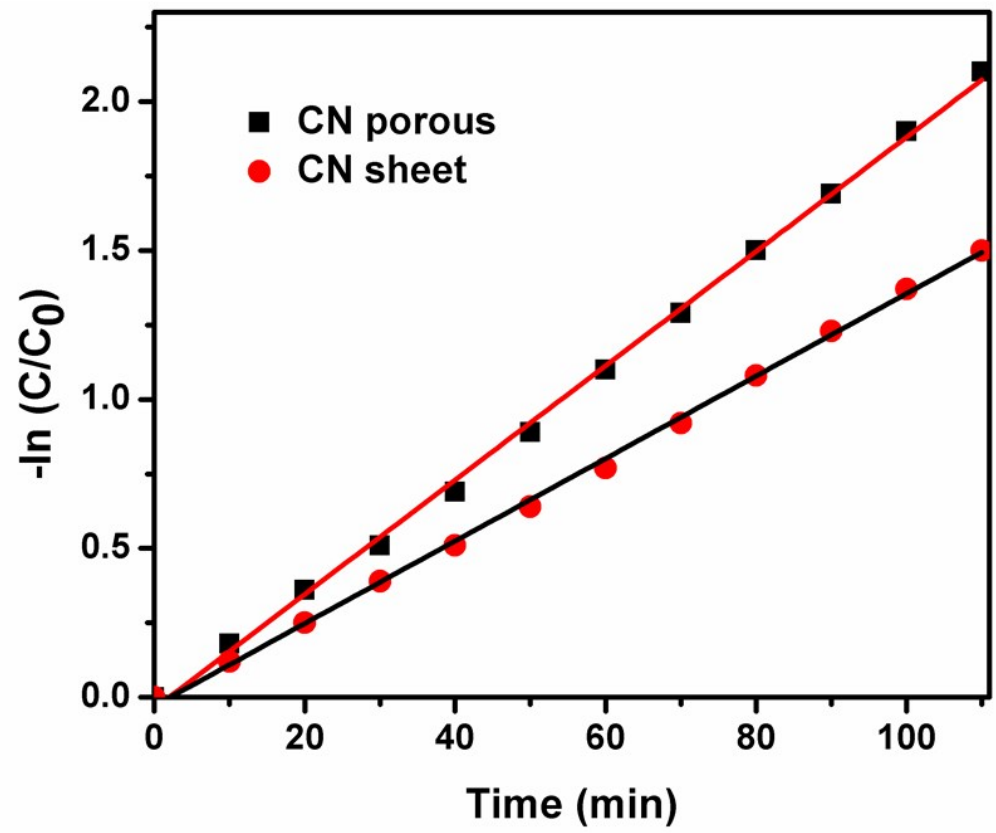

Fig.S5 Kinetics plots for CIP degradation using porous and sheet CN

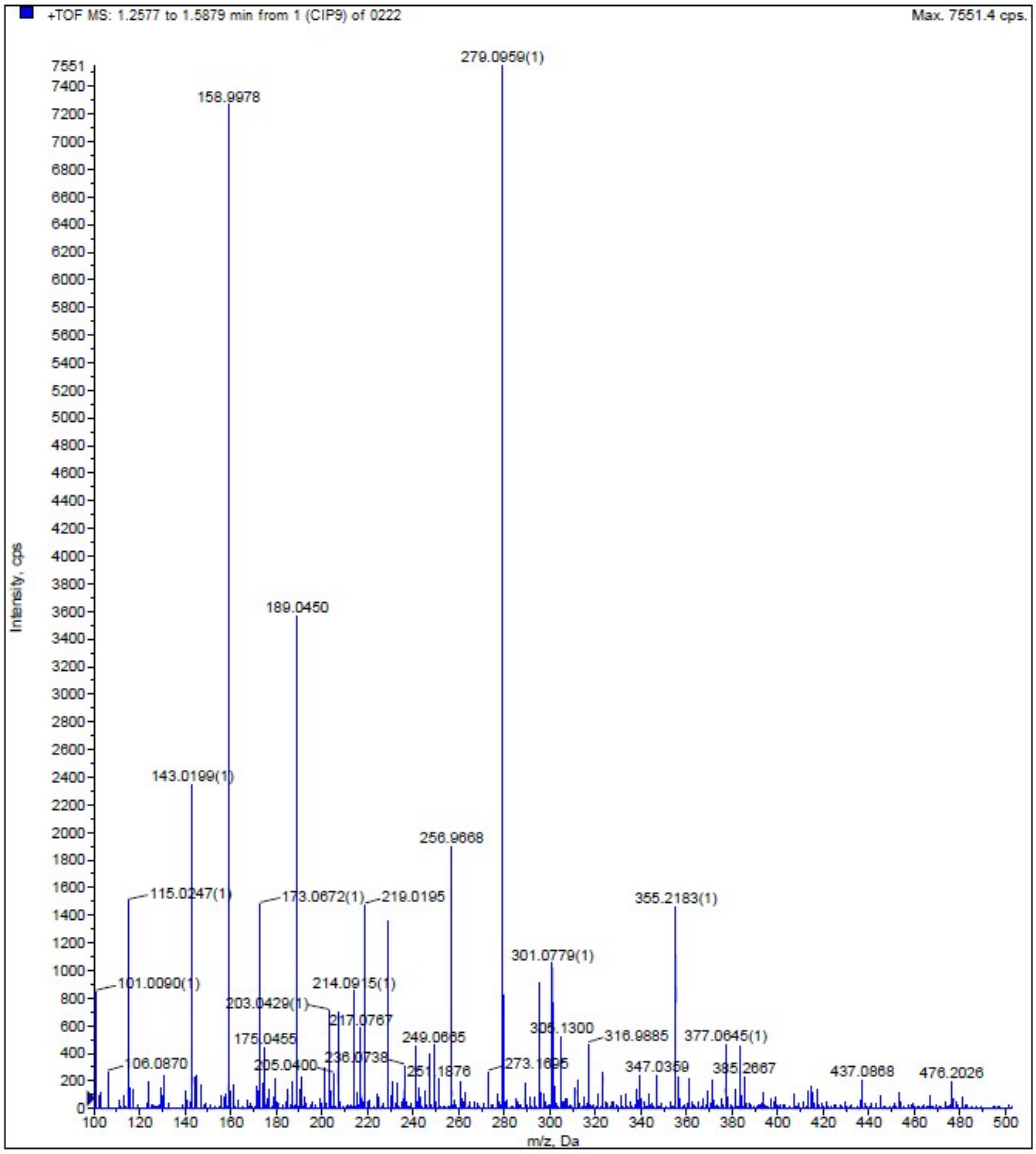
+TOF MS: 1.2577 to 1.5879 min from 1 (CIP9) of 0222
Max. 7551.4 cps.
Intensity, cps
m/z, Da
279.0959(1)
158.9978
189.0450
143.0199(1)
256.9668
115.0247(1)
173.0672(1)
219.0195
355.2183(1)
301.0779(1)
101.0090(1)
214.0915(1)
203.0429(1)
217.0767
305.1300
316.9885
377.0645(1)
175.0455
249.0665
106.0870
205.0400
236.0738
251.1876
273.1695
347.0359
385.2667
437.0868
476.2026

Fig. S6. LC-MS analysis of CIP degradation after 110 min using porous CN as photocatalyst.

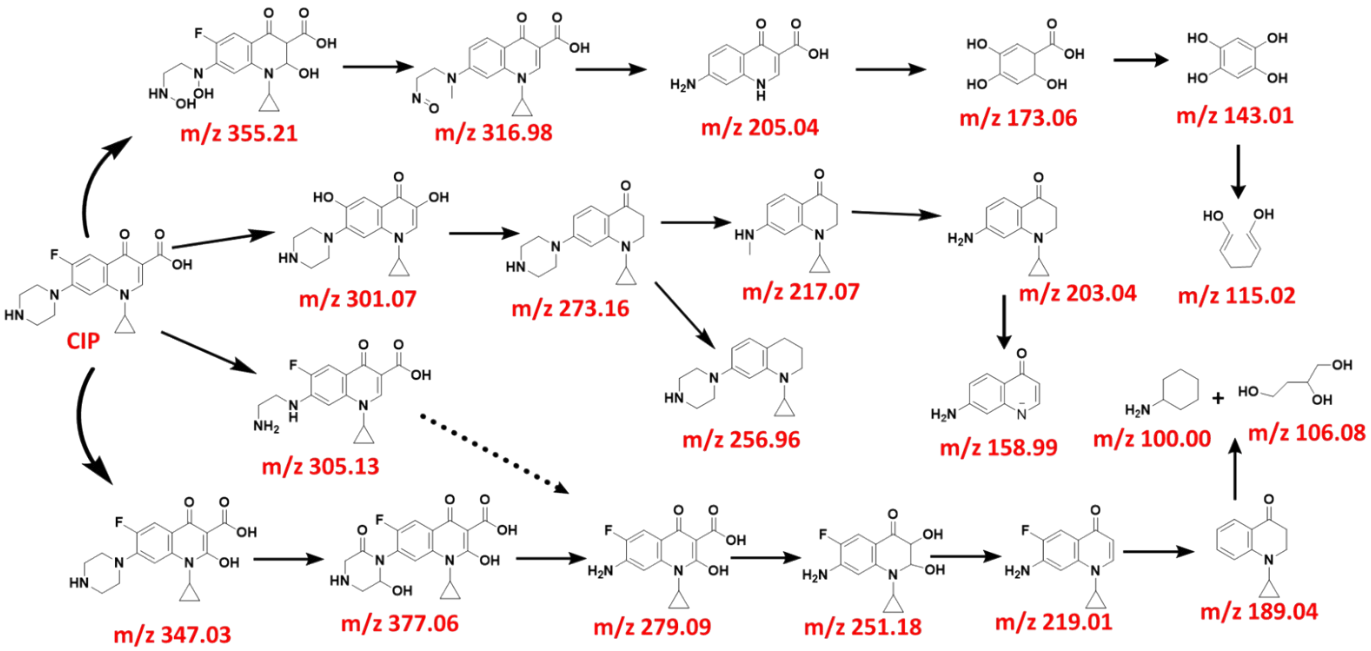

Scheme S1. The main degradation pathways of CIP over porous CN.

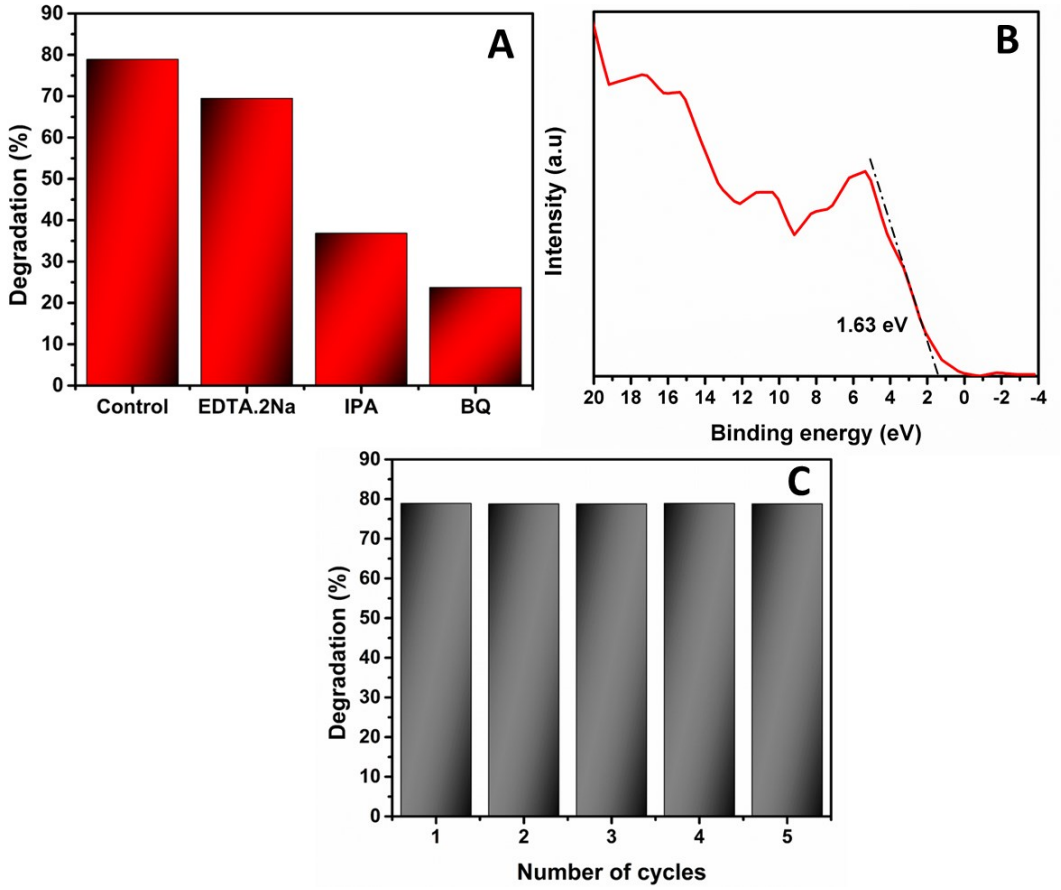

Fig. S7 (A) Photocatalytic degradation efficiency of CN porous structure during CIP degradation in the presence of various radical scavengers, **(B)** Valance band energy region of porous CN and **(C)** Photocatalytic degradation efficiency of CN porous structure during five cycles of CIP photocatalytic degradation.